Title
THEORY OF STRENGTHENING BY ORDERED PRECIPITATES

Author
Morris, J.W.

Publication Date
1986-02-01

UC-25
LBL-21156

To be presented at the
International Conference on
Aluminum Alloys,
Charlottesville, WV,
June 15-20, 1986

THEORY OF STRENGTHENING BY ORDERED PRECIPITATES

J. Glazer and J.W. Morris, Jr.

February 1986

Lawrence Berkeley Laboratory
University of California
Berkeley, California 94720

Prepared for the U.S. Department of Energy
under Contract DE-AC03-76SF00098

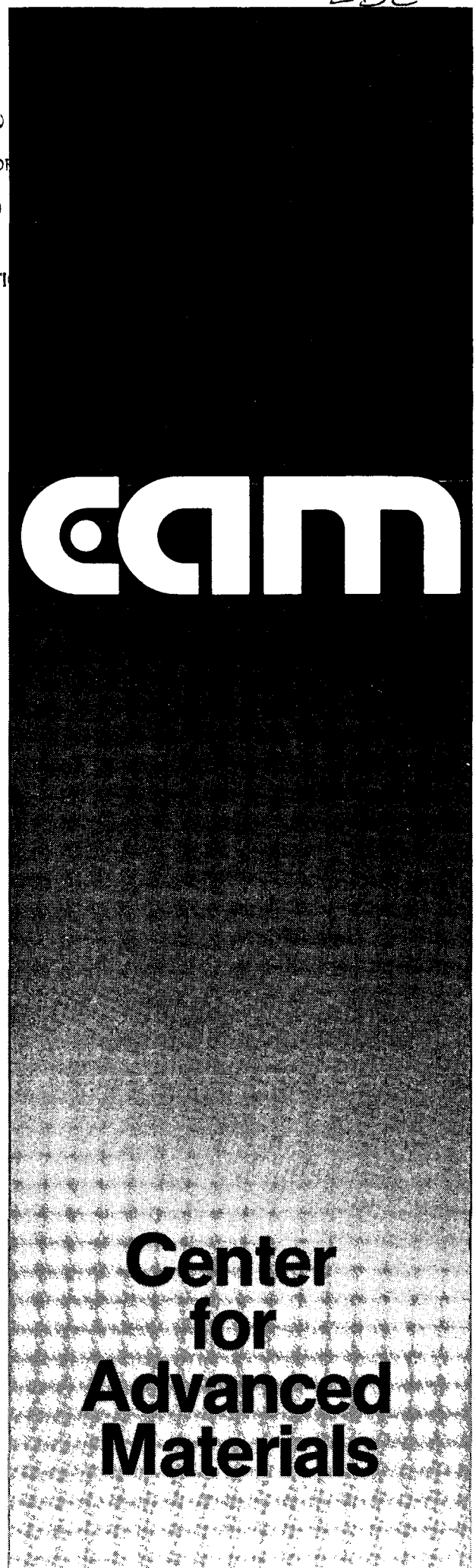

DISCLAIMER

THEORY OF STRENGTHENING BY ORDERED PRECIPITATES

J. Glazer and J.W. Morris, Jr.

Center for Advanced Materials,
Lawrence Berkeley Laboratory, and
Department of Materials Science and Mineral Engineering,
University of California, Berkeley

A model for the critical resolved shear stress near peak strength of alloys hardened by ordered precipitates is developed. The model is applied to the specific case of δ′ precipitates in binary aluminum-lithium alloys and found to be in good quantitative agreement with measured aging behavior. The effects of precipitate size, size distribution and shape on the critical resolved shear stress are explored via the model and predictions for more optimized microstructures presented.

INTRODUCTION

Most precipitation-hardened aluminum alloys are used at peak strength or in the slightly overaged condition. An understanding of the mechanistic sources of strength and yielding behavior is fundamental to defining desirable microstructures and designing processing steps to achieve them. In this paper, a model that is useful in this context is developed and some of its consequences explored.

Many factors influence the yield strength of precipitation-hardened alloys. Figure 1 is a schematic plot of the variation in yield strength of a typical precipitation hardened alloy as it is aged (often at elevated temperatures) over a period of time. A rapid initial increase in strength is observed, followed by a more gradual decline. The shape of the aging curve, the value of the peak strength, and the early deformation behavior are all known to vary with a wide variety of microstructural features, including precipitates, dislocations and solute atoms, the grain size and texture, the presence of precipitate free zones, etc.

Before the problem of understanding yielding behavior can be properly posed, an operational definition of yield strength is required. The yield stress is usually defined as the stress at which dislocations travel significant distances in the material, causing macroscopic deformation to take place. In a single crystal, the stress at which disloca-

tions glide freely is termed the critical resolved shear stress, τ_c. In a polycrystal, the yield stress σ_y is related to the critical resolved shear stress by the Taylor factor M (~ 3), which accounts for the fact that not all grains have favorably oriented slip planes and that material continuity must be preserved. The yield strength is related to the grain size and texture of the material through the parameter M. If the value of M is known for a particular grain structure, then the yield strength is fully determined by the critical resolved shear stress of the single crystal.

In single crystals, dislocation glide is restricted by obstacles in the material. Since the dislocation is both a crystallographic and an elastic defect, it interacts with and is impeded by any other crystallographic or elastic defect. Thus, solute atoms, other dislocations, and incoherent and coherent precipitates all act as obstacles to dislocation glide.

The purpose of this paper is to explain yielding behavior near peak strength in the context of a relatively simple model. The primary focus will be on the behavior of the critical resolved shear stress near peak strength in alloys hardened by coherent, ordered precipitates. Two important idealizations are implicit in this choice. First, studying the critical resolved shear stress rather than the yield strength itself is equivalent to neglecting the effects of grain size and texture. Second, narrowing the problem to the region near peak strength makes it reasonable to assume that relatively large precipitates provide most of the strength of the alloy. Hardening due to other obstacles and precipitate strengthening mechanisms that depend on a large surface-to-volume ratio may be neglected.

A model for the critical resolved shear stress near peak strength for alloys hardened by ordered precipitates is developed in the next section. The remainder of the paper focusses on the implications of the model to yielding behavior, specifically, the superposition of strengthening mechanisms, the effect of precipitate shape on strength, the shape of the aging curve, the prediction of yield strength data, the effect of the precipitate size distribution on strength. Finally, the model is used to predict yield strength data for binary aluminum-lithium alloys. Both the model and its consequences are discussed in greater detail in Glazer (1).

THE MODEL

An idealized single-crystal microstructure of a precipitation-hardened alloy is characterized in a mechanical sense by the forces associated with dislocation-precipitate interactions and in a geometric sense by the properties of the precipitates and their distribution, e.g. volume fraction, size, shape, size distribution, spacing, and distribution of spacings. (These geometric parameters are not all independent.) It is easiest to formulate a model for strengthening by separating the mechanical and geometric aspects of the problem. Since the deformation mode is qualitatively influenced by the strength of the dislocation-precipitate interaction, it will be considered first.

Precipitates harden the material through their interaction with dislocations. To glide over long distances, a dislocation must bypass precipitates that intersect its glide plane. When the dislocation runs into an array of obstacles it bows out between them as shown in Figure 2. If the applied shear stress resolved on the glide plane is great enough, then the dislocation loops or shears the obstacles. Athermal glide is assumed, since in precipitation-hardened alloys deformed at room temperature, the role of thermal activation is usually minimal.

Detailed models of dislocation-precipitate interactions exist. The most common simplifying assumptions are that

* isotropic elasticity applies,

* the dislocation is a flexible extensible string of constant line tension T for a given mean square obstacle spacing l_s,

* the precipitates may be simulated by point obstacles whose strength in athermal glide is given by F_s, the peak in the force-distance curve for the actual dislocation-precipitate interaction (see Figure 3 for an example).

When the dislocation bows out between precipitates under an applied stress, it exerts a force on each obstacle given by the component of the line tension in the direction of motion. The force from the dislocation F_d is related to the angle of bowout, and is given for the geometry of figure 2 by

$$F_d = 2T\cos(\Psi/2) \tag{1}$$

The maximum force the dislocation can exert on the obstacle (ignoring the lowering effect of any dislocation self-interactions) occurs when $\Psi = 0$, or

$$F_d^{max} = 2T \tag{2}$$

In this configuration the two arms of the dislocation are antiparallel and annihilate, forming a loop around the precipitate and allowing the dislocation to move on. This phenomenon is referred to as Orowan looping.

If F_d exceeds F_s before looping occurs, the dislocation shears the precipitate. It should be clear from this discussion that for constant line tension T, the angle $\Psi/2$ (or $\cos \Psi/2$) at which the precipitate is bypassed (either sheared or looped) defines its strength. It is convenient to describe the precipitate strength by the dimensionless variable β given by

$$\beta = F/2T = \cos(\Psi/2) \tag{3}$$

The geometry of the problem is largely contained in statistical solutions to the model for the critical resolved shear stress for a random array of obstacles. A solution that has been used successfully in the past to model the critical resolved shear stress ((1), Glazer et al (2), Melander (3), Melander and Persson (4, 5)) was proposed by

Hanson and Morris (6, 7). Its chief elements may be summarized as follows:

* The configuration of the dislocation is described by a unique set of pinning points. The critical resolved shear stress of the array is reached when the dislocation bypasses the weakest point in the strongest configuration.

* For a random array of identical obstacles the critical resolved shear stress is statistically determined. It is convenient to define a dimensionless critical resolved shear stress

$$\tau^* = \tau l_s b/2T \tag{4}$$

where l_s is the mean square obstacle spacing and b is the Burgers' vector in the glide plane. The analytic solution for the critical resolved shear stress is then given by

$$\tau^* = 0.9\beta^{3/2} \tag{5}$$

* The critical resolved shear stress for a mixture of obstacle types is a quadratic sum

$$\tau^2 = \Sigma\, x_\alpha(\tau_\alpha)^2 \tag{6}$$

where x_α is the fraction of obstacles of type α and τ_α is the critical resolved shear stress for an array containing obstacles of type α only.

Quantifying this model requires an understanding of the sources of the shear strength of the precipitate, F_s. A number of interactions between the dislocation and the precipitate have been proposed at one time or another (Ardell, (7)). These include chemical strengthening (caused by the additional interface created when the precipitate is sheared), modulus strengthening (caused by the difference in modulus between the precipitate and the matrix), stacking fault strengthening (caused by the difference in stacking fault energy between the precipitate and the matrix), order strengthening (caused by the antiphase boundary created by the passage of a dislocation through an ordered precipitate) and coherency strengthening (caused by the interaction of the elastic field of a dislocation and the misfit strain associated with a coherent precipitate). Only order and coherency strengthening are likely to be important for coherent, ordered precipitates of reasonable size.

To simplify the discussion even further, we specialize to the case of order hardening. Spherical precipitates are assumed unless otherwise specified. In this case a number of additional assumptions about the manner in which the precipitates strengthen the material are valid:

* The maximum effective radius of a precipitate is the minimum radius at which precipitates are looped rather than sheared. This size may be determined experimentally, and is termed the looping radius, r_{loop}.

* Each precipitate may be reduced to a set of point obstacles whose strengths correspond to the effective radii of the precipitate in the glide planes that intersect it.

* The strength of the precipitate is assumed to be a function of the effective radius of the precipitate only.

* Because the precipitates are ordered, the dislocations that shear them are coupled by the antiphase boundary created by the first dislocation. In the $L1_2$ structure (e.g. δ' in aluminum-lithium alloys or γ' in nickel-based superalloys), order is restored by the second dislocation, so the dislocations travel in pairs as superdislocations. This coupling has the consequence that the critical resolved shear stress predicted by the model will be twice the applied stress at yielding.

IMPLICATIONS

The model described in the previous section is relatively simple. However, it leads to a number of useful qualitative predictions. This section will provide several examples that illustrate the utility of the model for order-hardened systems. For model systems for which its approximations are fairly good (e.g. binary aluminum-lithium alloys), these predictions can be made more quantitative.

Superposition of precipitate strengthening mechanisms

Figure 3 illustrates the manner in which various dislocation-precipitate interactions combine to determine the strength of the precipitate in athermal glide. The strength is determined only by the peak in the force-distance curve. If various interactions (for instance, coherency and order) are spatially displaced, then the total strength is not the sum of peaks of the individual interactions, but the maximum value of the total interaction force. As a result, increasing one source of strength, for instance the misfit, may or may not have a significant effect on the strength of the alloy, depending on what other strengthening mechanisms are operative.

Strength of plate-like precipitates

Plate-like precipitates are usually observed when the misfit strain in the habit plane is relatively high, while spherical precipitates are generally observed when it is low. High-strength alloys are usually hardened by plate-like precipitates. The increase in strength is partially due to the high misfit strain and its localization at the perimeter of the plate, but it can also be shown that increased strengthening should be observed on purely geometric grounds.

Because the plate distributes the precipitated material more efficiently, a higher strength is predicted even if the misfit strain is ignored. Figure 4 shows a spherical precipitate and a plate-like (disc-shaped) precipitate of equal volume. Since strengthening in athermal glide is determined entirely by the maximum in the force-distance relation for the precipitate-dislocation interaction, the plate strengthens much more efficiently. It provides both more obstacles, because it

intersects more glide planes, and stronger obstacles because the width of the plate face is larger than the diameter of the sphere of equivalent volume. The misfit strain around the plate could be included in the model by considering the effective size of the plate to be increased.

Volume fraction effects

The precipitate volume fraction f appears in the equation for the critical resolved shear stress through the mean square obstacle spacing l_s. It can be shown easily that the critical resolved shear stress is proportional to $f^{1/2}$. Consequently, any significant increase in the precipitate volume fraction during aging will be reflected in increased strength.

The change in volume fraction during precipitate coarsening can be estimated on thermodynamic grounds. The impetus for the increase is the precipitate-matrix interface, whose energy alters the equilibrium between the matrix and precipitate phases (Porter and Easterling (8)). The requirement of mechanical equilibrium across the curved interface leads to a pressure difference

$$\Delta P = 2\gamma_s/r \tag{7}$$

where γ_s is the surface energy of the interface. The pressure difference decreases the magnitude of the free energy change for the reaction by the amount

$$\Delta G_\gamma = V\Delta P \tag{8}$$

As the precipitate radius increases during coarsening, the free energy change due to the interface decreases in magnitude, resulting in further precipitation of the second phase and decreased solubility of the solute species.

Although the increase in volume fraction during coarsening can be substantial, the effect is almost entirely confined to small precipitates. Consequently, it is of little importance near peak strength. Quantitative results for the binary aluminum-lithium system are discussed later.

Aging curves

The overall shape of the aging curve can be predicted by dimensional analysis of equations (4) and (5). Both hardening and softening are expected as a result of precipitate coarsening at constant volume fraction. In the underaged condition, the precipitates are sheared by the matrix. Since both F_s and l_s are proportional to the maximum cross-section of the precipitate in the glide plane, the critical resolved shear stress is proportional to $r^{1/2}$, and strengthening is observed. In the overaged condition, the precipitates are looped by the dislocation. The force for looping F_d is roughly constant with precipitate size. Since l_s is still proportional to the precipitate radius, the critical resolved shear stress is proportional to r^{-1}, and the material softens rapidly with continued coarsening. If all the obstacles were the same

strength (highly unlikely in any real material), peak strength would occur when the precipitates reached the looping radius.

Advantages of uniform precipitate size

As mentioned previously, a precipitate can be represented as a series of mathematical obstacles whose strengths correlate to the effective radii of the precipitate on the glide planes it intersects. Thus, a distribution of obstacles sizes can be generated for a given precipitate size distribution. The obstacle size distribution, together with the looping radius, can be used to calculate the critical resolved shear stress.

The value of the critical resolved shear stress depends more strongly on precipitate radius after looping begins than before. Consequently, if a distribution of precipitate sizes exists, peak strength will occur almost immediately after the largest of the precipitates reaches the looping radius, not when the average sized precipitate reaches the looping radius. By contrast, the amount of strengthening provided by the precipitates is most closely related to the average precipitate radius. As a result, the maximum achievable strength increases as the precipitate size distribution narrows. As illustrated in figure 5, when the largest precipitates reach the looping radius, the average precipitate radius of a narrow distribution is greater than the average radius for a broad distribution. The strength of the narrow distribution is correspondingly higher. The magnitude of this effect for experimentally measured precipitate size distributions in binary aluminum-lithium alloys is estimated in (2).

Prediction of experimental data for aluminum-lithium alloys

The binary aluminum-lithium system is an excellent model system for the critical resolved shear stress solution proposed here for a number of reasons:

* The strengthening precipitate Al_3Li, (δ') is spherical, so an obstacle distribution is easily generated. Because of the intense industrial interest in this system, a great deal of experimental data exists, including aging curves for experimentally measured precipitate size distribution.

* The precipitate-matrix surface energy is relatively low, so the assumption that coarsening occurs at constant volume fraction is good. The cumulative change in precipitate volume fraction during coarsening for δ' precipitates in aluminum is shown in figure 6. Most of the increase occurs while the precipitates are less than 20b in diameter; the increase is negligible near peak strength ($> 100b$). (The matrix Burgers' vector is 0.29 nm).

* The δ' precipitate size distribution coarsens self-similarly at a constant rate, the Lifshitz-Slyozov-Wagner coarsening rate constant (Gu, et al (9)).

* The misfit strain of the precipitate is extremely low, so the assumption that strengthening is dominated by order hardening is a good

one.

* The δ′ has the $L1_2$ crystal structure, so dislocations, move in coupled pairs. The effect of the coupling is to halve the stress required for yielding. Screw dislocations have been observed to control yielding (Miura et al, (10)).

* The looping radius has been measured by several investigators; a reasonable estimate for the looping radius is 30 nm for $l_s \sim 1$ μm (de Hosson et al (11), Sainfort and Guyot (12)).

To make the calculations more accurate numerically, the model described in this paper was modified slightly (1,2). Dislocation self-interactions were included by setting the maximum value of β at 0.7 and making the line tension proportional to ln (l_s).

The results for an Al-2.78Li-0.3Mn alloy aged at 200°C are shown in figure 7. The experimental data is taken from (9). Since the quenched alloy undoubtedly contains some atom clusters, the theoretical aging curve has been shifted to slightly shorter aging times to obtain the best fit. To convert the theoretical values of the critical resolved shear stress to yield strength, a Taylor factor of 3 was assumed. The strength increment for both yield strength curves was taken as the strength above the lowest measured strength. The figure shows that the theoretical and experimental aging curves are in excellent agreement up to peak strength. The rapid fall of the theoretical curve below the experimental one after peak strength is not surprising, since the model does not account for the uncoupling of superdislocations observed when Orowan looping becomes important (10, 12). The theoretical aging curve for a uniform distribution of precipitates at the same volume fraction is shown for comparison.

ACKNOWLEDGEMENTS

This work was supported by the Director, Office of Energy Research, Office of Basic Energy Sciences, Materials Sciences Division of the U.S. Department of Energy under Contract No. DE-AC03-76SF00098. One of the authors, J. Glazer, was supported by an ATT Bell Laboratories Fellowship.

REFERENCES

(1) Glazer, J., M.S. Thesis, University of California, Berkeley, 1986.

(2) Glazer, J., Edgecumbe, T.S. and Morris, J.W., Jr., "A Theoretical Analysis of the Aging Response of Al-Li Alloys Strengthened by Al_3Li Precipitates," Proceedings of the Third International Aluminum-Lithium Conference, Oxford, England, 1985, in press.

(3) Melander, A., Scand. J. Metall., Vol. 7, 1978, p. 109.

(4) Melander, A. and Persson, P.Å., Acta Met., Vol. 26, 1978, p. 267.

(5) Melander, A. and Persson, P.Å., Metal Science, Vol. 12, 1978, p.391.

(6) Hanson, K. and Morris, J.W., Jr., J. Appl. Phys., Vol. 46, 1975, p. 983 and p. 2378.

(7) Ardell, A.J., Met. Trans. A, Vol. 16A, 1985, p. 2131.

(8) Porter, D.A. and K.E. Easterling, "Phase Transformations in Metals and Alloys," Van Nostrand Reinhold Co. Ltd., Berkshire, England, 1981.

(9) Gu, B.P., Liedl, G.L., Sanders, T.H., Jr., Welpmann, K., Mat. Sci. and Eng., Vol. 76, 1985, p. 147.

(10) Miura, Y., Matsui, A., Furukawa, M. and Nemoto, M., "Plastic Deformation of Al-Li Single Crystals," Proceedings of the Third International Aluminum-Lithium Conference, Oxford, England, 1985, in press.

(11) Sainfort, P. and Guyot, P., "Fundamental Aspects of Hardening in Al-Li and Al-Li-Cu Alloys," Proceedings of the Third International Aluminum-Lithium Conference, Oxford, England, 1985, in press.

(12) DeHosson, J. Th. M., Huis in't Veld, A., Tamler, H. and Kanert, O., Acta Met., Vol. 32, 1984, p. 1205.

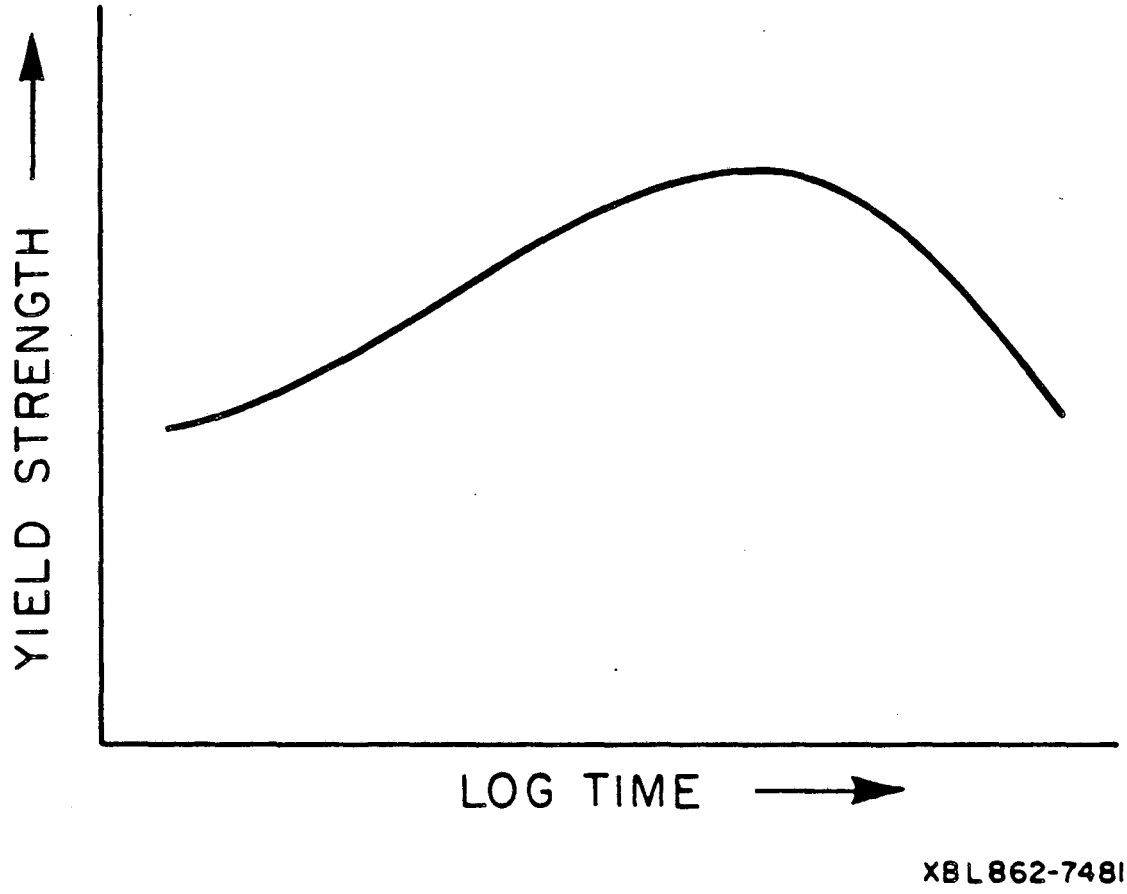

Figure 1 Schematic aging curve

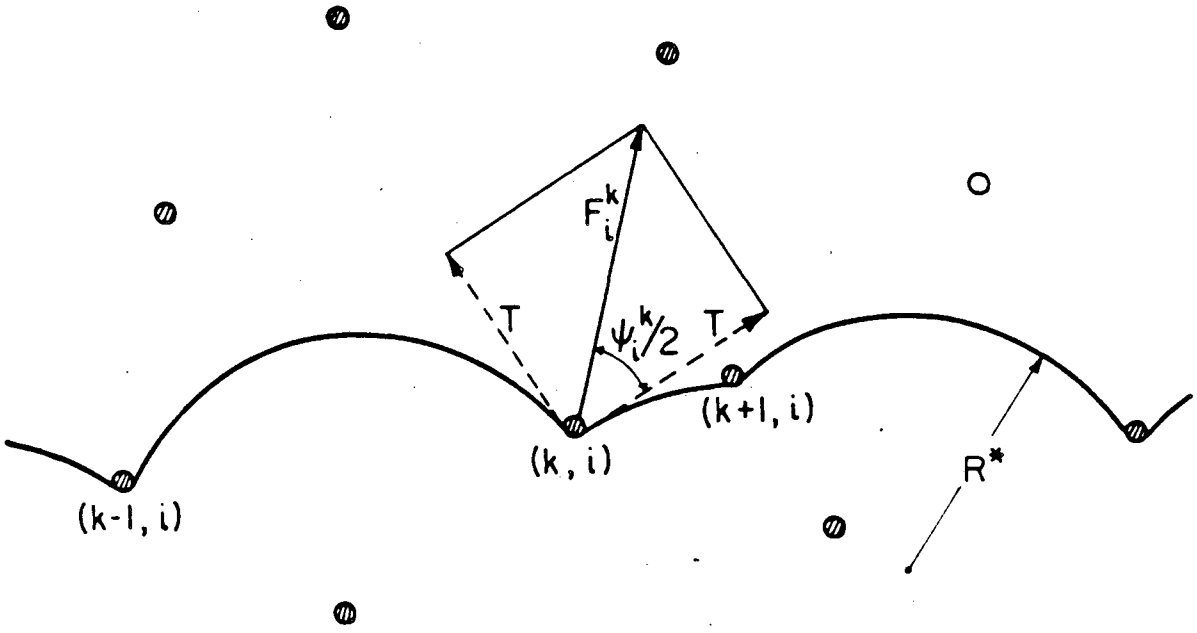

Figure 2 Dislocation bow-out under stress between point obstacles

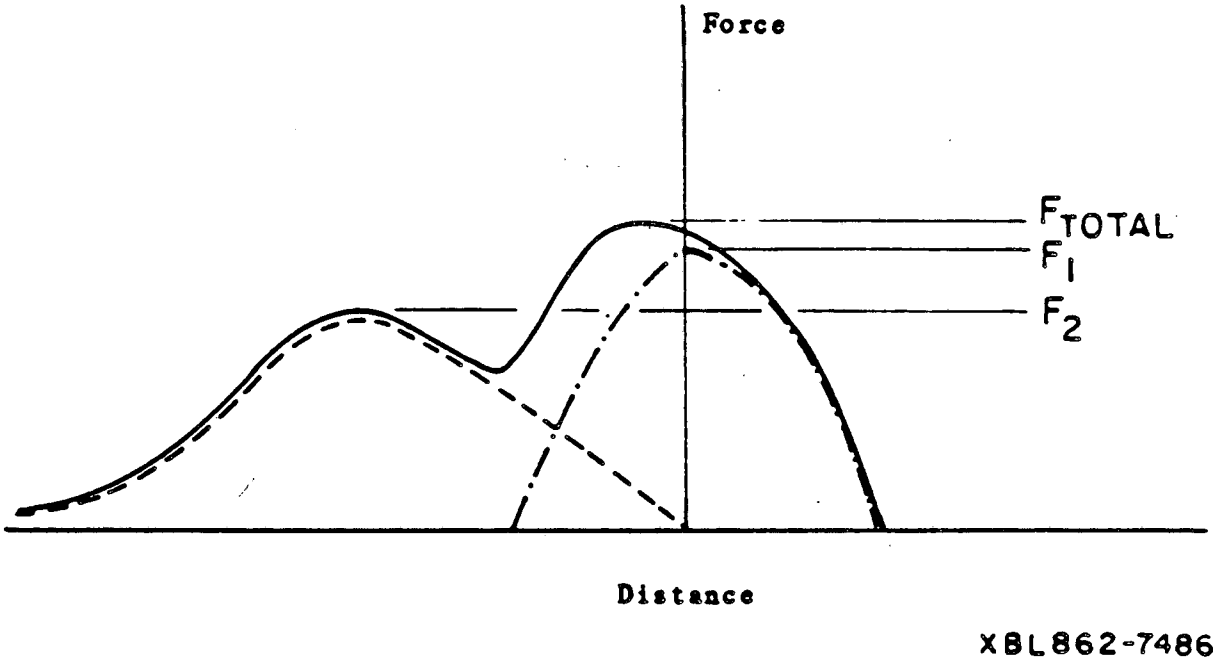

Figure 3 Force-distance curve illustrating superposition of precipitate strengthening mechanisms

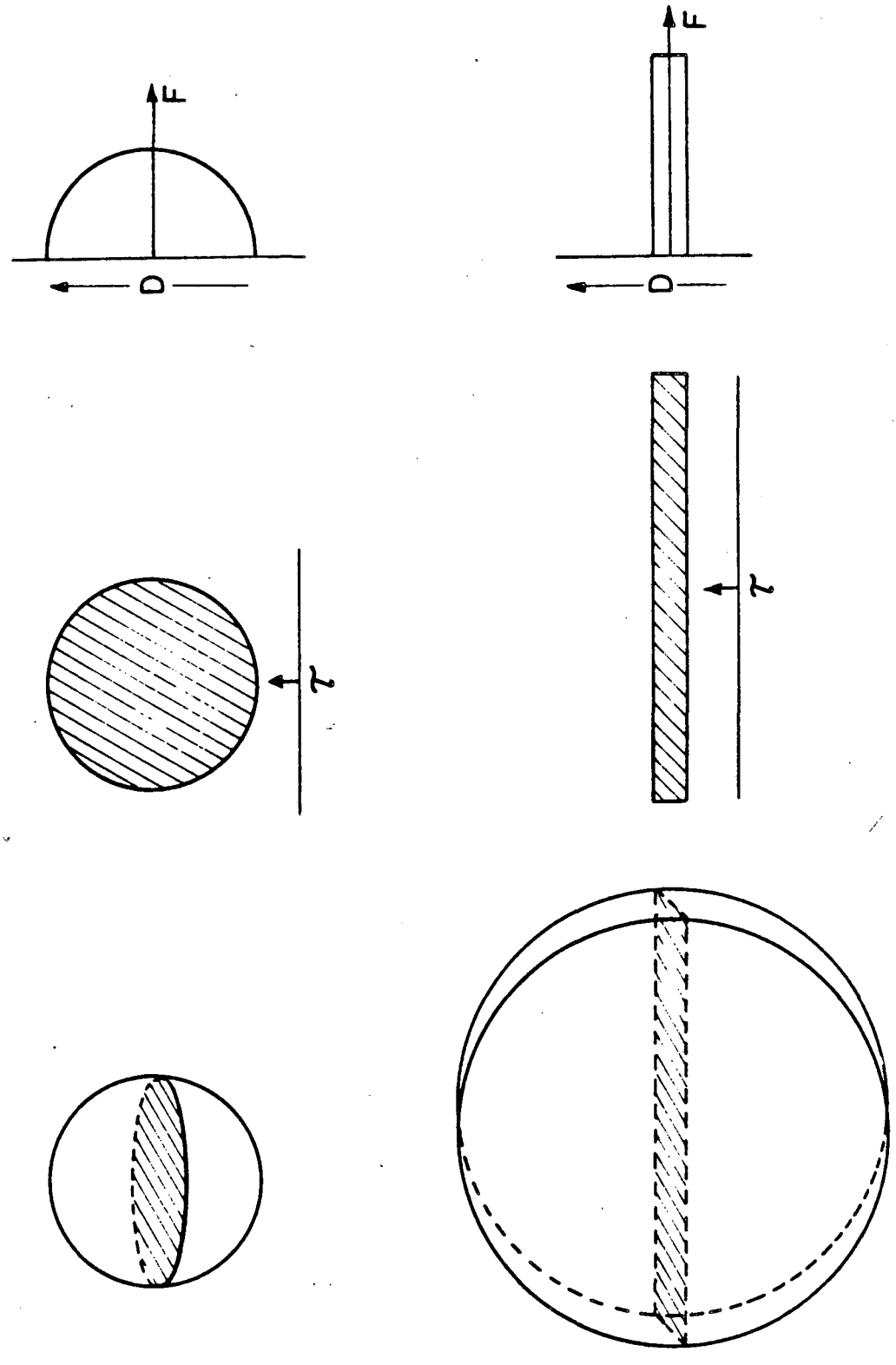

Figure 4 Comparative strengthening from spherical and plate-like precipitates with equal volume

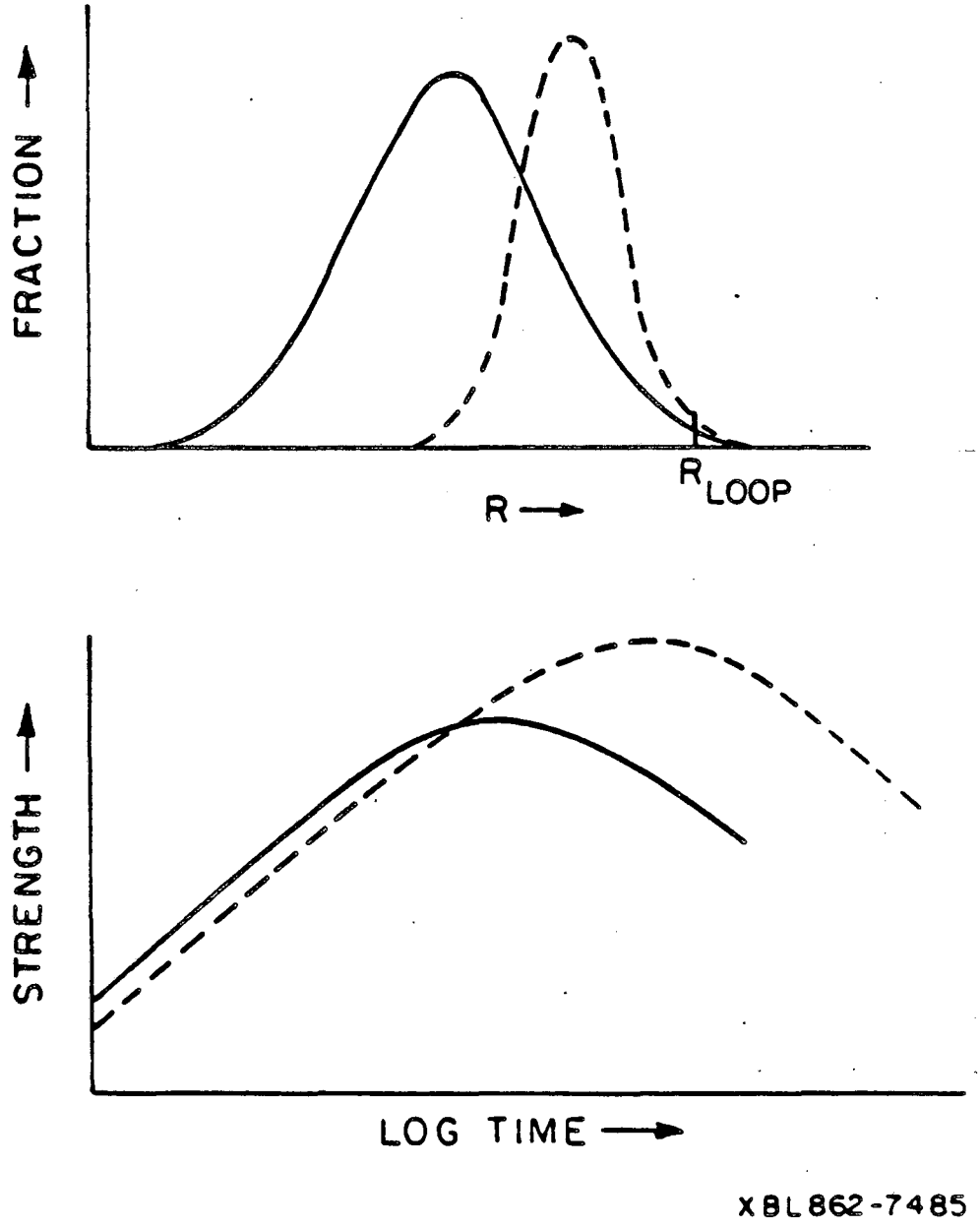

Figure 5 Advantage of a narrow precipitate size distribution

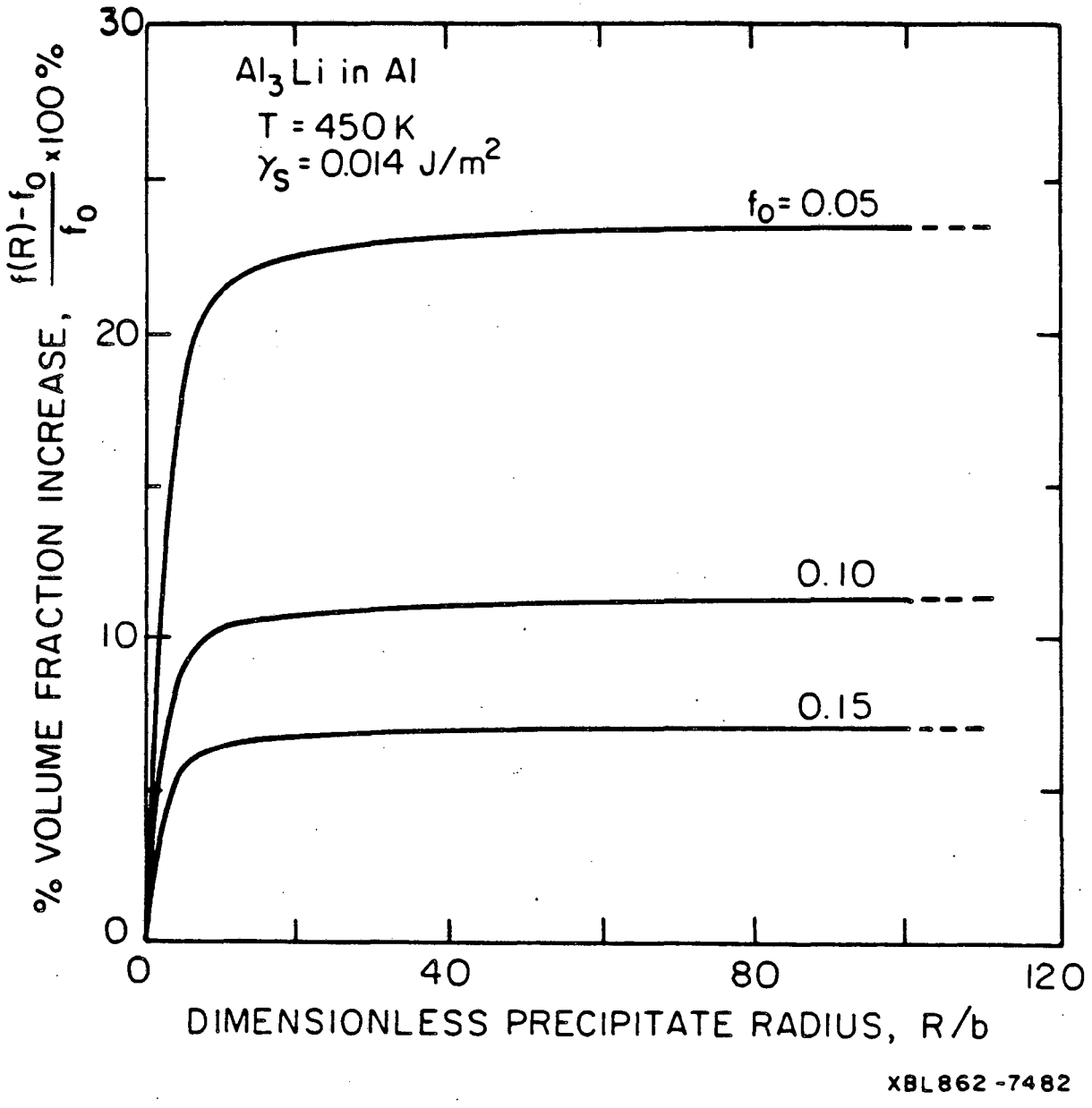

Figure 6 Cumulative change in precipitate volume fraction during coarsening for Al_3Li precipitates in Al

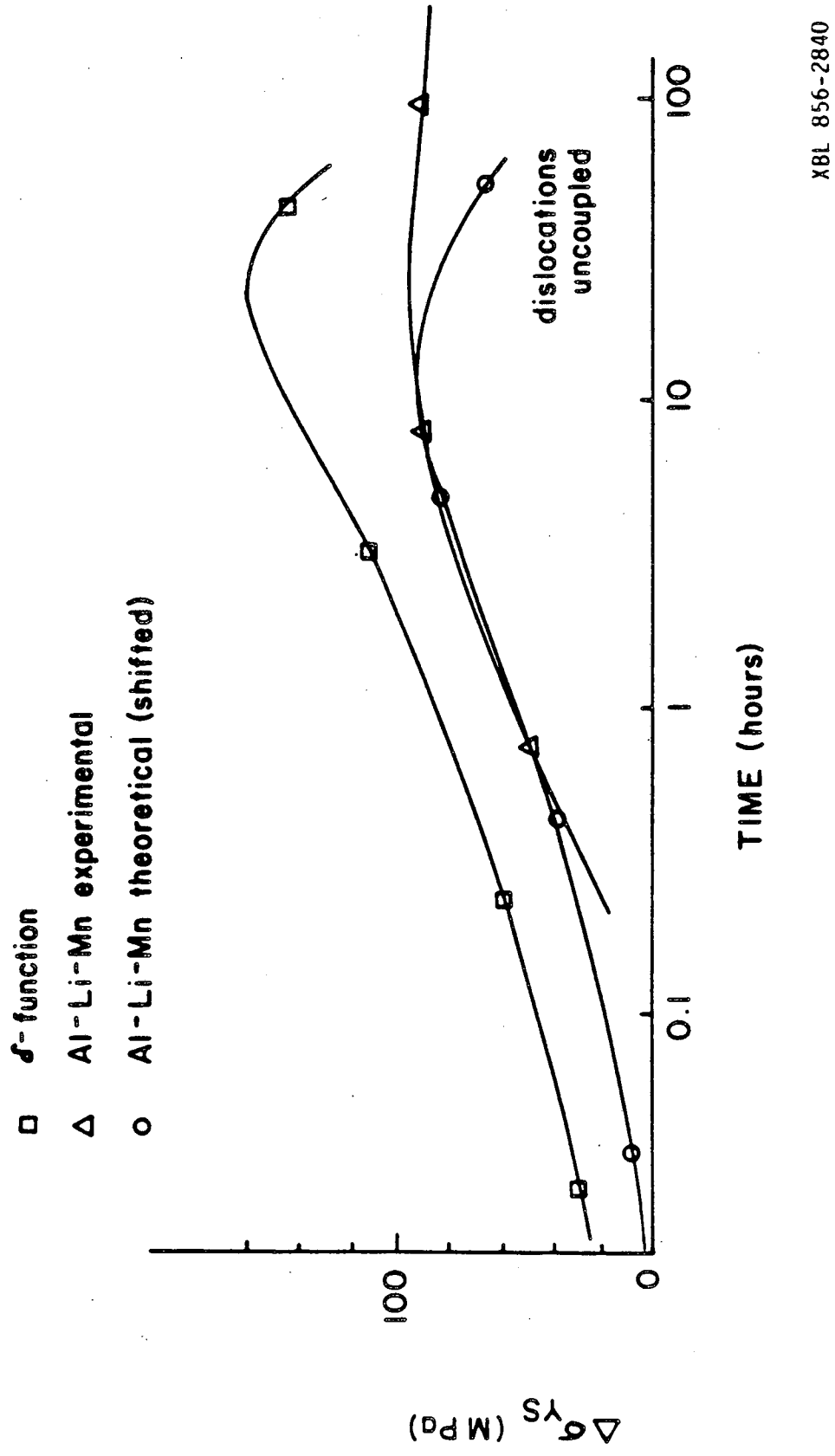

Figure 7 Prediction of experimental aging curve

This report was done with support from the Department of Energy. Any conclusions or opinions expressed in this report represent solely those of the author(s) and not necessarily those of The Regents of the University of California, the Lawrence Berkeley Laboratory or the Department of Energy.

Reference to a company or product name does not imply approval or recommendation of the product by the University of California or the U.S. Department of Energy to the exclusion of others that may be suitable.

TECHNICAL INFORMATION DEPARTMENT
LAWRENCE BERKELEY LABORATORY
UNIVERSITY OF CALIFORNIA
BERKELEY, CALIFORNIA 94720